Transient receptor potential cation channel, subfamily C, member 5 (TRPC5) is a cold-transducer in the peripheral nervous system

Katharina Zimmermann[a,b,1,2], Jochen K. Lennerz[a,c,d,1,3], Alexander Hein[a,1,4], Andrea S. Link[e], J. Stefan Kaczmarek[a,b], Markus Delling[a], Serdar Uysal[a], John D. Pfeifer[c], Antonio Riccio[a], and David E. Clapham[a,b,f,5]

Departments of [a]Cardiology, Manton Center for Orphan Disease, and [b]Neurobiology, Harvard Medical School, Boston, MA 02115; [c]Department of Pathology and Immunology, Washington University, St. Louis, MO, 63110; [d]Department of Pathology, Massachusetts General Hospital/Harvard Medical School, Boston, MA, 02116; [e]Department of Physiology and Pathophysiology, University Erlangen, 91054 Erlangen, Germany; and [f]Howard Hughes Medical Institute, Harvard Medical School, Children's Hospital Boston, Boston, MA 02115

Contributed by David E. Clapham, September 20, 2011 (sent for review August 9, 2011)

Detection and adaptation to cold temperature is crucial to survival. Cold sensing in the innocuous range of cold (>10–15 °C) in the mammalian peripheral nervous system is thought to rely primarily on transient receptor potential (TRP) ion channels, most notably the menthol receptor, TRPM8. Here we report that TRP cation channel, subfamily C member 5 (TRPC5), but not TRPC1/TRPC5 heteromeric channels, are highly cold sensitive in the temperature range 37–25 °C. We found that TRPC5 is present in mouse and human sensory neurons of dorsal root ganglia, a substantial number of peripheral nerves including intraepithelial endings, and in the dorsal lamina of the spinal cord that receives sensory input from the skin, consistent with a potential TRPC5 function as an innocuous cold transducer in nociceptive and thermosensory nerve endings. Although deletion of TRPC5 in 129S1/SvImJ mice resulted in no temperature-sensitive behavioral changes, TRPM8 and/or other menthol-sensitive channels appear to underpin a much larger component of noxious cold sensing after *TRPC5* deletion and a shift in mechanosensitive C-fiber subtypes. These findings demonstrate that highly cold-sensitive TRPC5 channels are a molecular component for detection and regional adaptation to cold temperatures in the peripheral nervous system that is distinct from noxious cold sensing.

pain | single-fiber | thermo-transient receptor potential | nociception | temperature sensing

Nociceptors and thermoreceptive neurons, such as cold and heat receptors, innervate the skin and deep tissues. The cell bodies of sensory nerve endings are clustered in ganglia located in the vertebral column and cranium. Their projections extend to the skin where they arborize in terminals embedded between keratinocytes. Although nociceptors are polymodal and respond to stimuli (cold, heat, pressure, and noxious chemicals) that are capable of producing tissue damage and pain (1), cold receptors are unimodal and specialized to detect cool and cold temperatures (2). Transient receptor potential (TRP) ion channels are principal transducers of thermal stimuli that depolarize nerve terminals to the action potential threshold. Action potentials then relay the sensory information to integrative centers in the spinal cord and brain.

All proteins are temperature sensitive, but most ion channels exhibit two- to threefold increases in gating with a 10 °C change in temperature (Q_{10} = 2–3). Certain ion channels exhibit dramatic temperature sensitivity in gating over physiologically relevant ranges (Q_{10} = 10–30). Mammalian ion channels with such high Q_{10} values include particular two-pore K^+ channels (3), the voltage-gated proton channel (4), transient receptor potential cation channel subfamily V members 1–3 (TRPV1–3) (5–7), transient receptor potential menthol receptor 8 (TRPM8) (8), and in some reports, TRP cation channel subfamily A member 1 (TRPA1) (9, 10). There is no a priori requirement for cold encoding by high Q_{10} channels—action potential firing rates are affected perforce by temperature, even if driven solely by conventional Na_V and K_V channels—but high Q_{10} channels are likely suspects in encoding temperature changes. Although TRPM8 (a menthol receptor) is generally considered the primary cold sensor for innocuous cold (11–13), and TRPA1 participates in noxious cold sensing (9, 10) (14), many cold-sensitive neurons lack TRPM8 as well as TRPA1 (15).

Results

TRPC5 Is Potentiated by Cooling. We conducted a search for cold sensitivity across the canonical TRP channel subfamily (TRPC) (16). TRPC channels were expressed heterologously in HEK293 cells stably expressing the muscarinic type 1 receptor (HM1-HEK293), and whole-cell currents were recorded in response to cold stimulation. As for many other TRP channels (17), TRPC5 is constitutively active at ambient temperature in heterologous expression systems, is sensitive to internal Ca^{2+}, and is potentiated by phospholipase C (PLC)-coupled receptor activation (18). Surprisingly, we found that TRPC5 current (I_{TRPC5}) increased as temperature cooled below 37 °C, peaking around 25 °C at negative membrane potentials. Cold-induced activation of TRPC5 current was potentiated by activation of Gq-linked HM1 via carbachol as well as by PLC activation via extracellular lanthanum (La^{3+}). The cold-activated current was constant over a large range of physiologically relevant membrane potentials (−40 to −80 mV). Ca^{2+}-imaging experiments confirmed a cold-induced increase in intracellular Ca^{2+} following PLC activation only in TRPC5-transfected HM1 cells (Fig. 1 *A–H*).

Unlike TRPM8, which inactivates over time at a constant temperature (19), TRPC5 does not inactivate significantly in persistent colder temperatures. Also, unlike TRPM8, TRPC5 is not activated by menthol in our heterologous expression system (Fig. S1) and thus can be separated easily from TRPM8. As we have shown previously, TRPC1 can heteromerize with TRPC5 and, although also potentiated by La^{3+} and PLC activation, the current–voltage (I–V) curves are quite distinct (20). In addition, TRPC1/C5 heteromers are confined to the cell body, whereas TRPC5 homo-
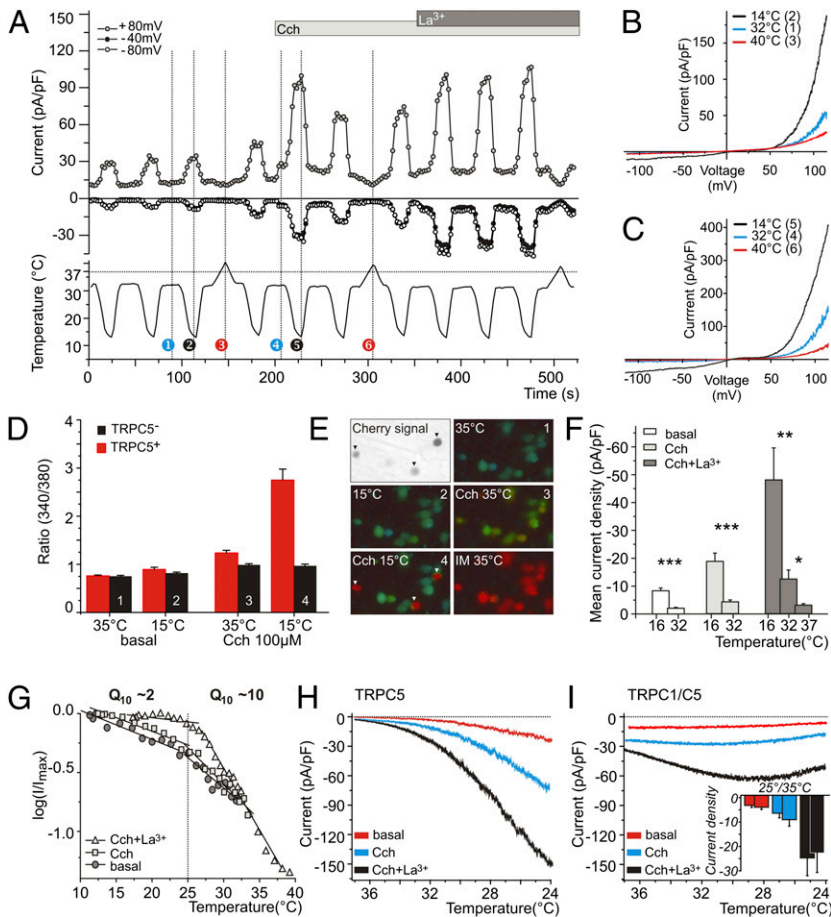
Fig. 1. Cooling potentiates TRPC5 current. (*A*) Whole-cell currents of an HM1-HEK293 cell expressing mouse TRPC5. Circles represent current amplitudes derived from 400-ms voltage ramps (−120 to +120 mV) applied at 2.4-s intervals (holding potential: gray circles, +80 mV; black circles, −40 mV; white circles, −80 mV). Cooling from 32–14 °C increased I_{TRPC5}, whereas warming to 40 °C decreased I_{TRPC5}. Carbachol (Cch; 100 μM) or La^{3+} (100 μM) activated and sensitized the current to cold. Bars indicate duration of agonist application. Numbers in circles correspond to I–V traces in *B* and *C*. (*B* and *C*) I–V relationship at three different temperatures for basal (*B*) and Cch-activated (*C*) currents. (*D*) Averaged Ca^{2+} in TRPC5-transfected (TRPC5$^+$, red bars) and TRPC5-non-transfected (TRPC5$^-$, black bars) HM1-HEK293 cells in response to cold and Cch, measured using fura2-AM (*n* = 45 each). (*E*) Representative images from calcium imaging. *Top Left* to *Bottom Right*: Cherry-FP signal illustrates transfection of HM1-HEK293 cells with TRPC5 (arrowheads); basal Ca^{2+} signal using fura2-AM; numbers 1–4 correspond to conditions as marked in the column pairs in *D*; ionomycin (IM) highlights maximum Ca^{2+} in all cells. (*F*) Averaged current densities at 40 mV. (*G*) A cell was cooled at a rate of 0.5 °C/s, and I/I$_{max}$ was plotted vs. temperature. The highest temperature sensitivity was between 37–25 °C (Q$_{10}$ ~10). *P < 0.01; **P < 0.001; ***P < 0.00001, *n* = 8–22, Student's *t* test. See also [SI Materials and Methods](#). (*H*) Current–temperature relationship for TRPC5 at −40 mV. (*I*) Current–temperature relationship for TRPC1/C5 heteromeric channels at −40 mV. TRPC1/C5 heteromers are not cold sensitive. (*Inset*) Heteromeric current densities at 25 °C and 35 °C; *n* = 5.

mers are transported down neurite processes to growth cones and nerve terminals where they can be exposed to changes in temperature (20–22). In contrast to TRPC5 homomeric channels, cooling did not enhance TRPC1/5 heteromeric current (Fig. 1*I*), and thus we focused on TRPC5 homomeric channels.

TRPC5 in Peripheral Nerves, Dorsal Root Ganglion, and the Spinal Cord Dorsal Horn. We applied previously characterized antibodies ([Table S1](#)) to tissue sections and confirmed the presence of TRPC5 in murine dorsal root ganglion (DRG) neurons (Fig. 2*A*), consistent with previous reports (23). We confirmed the presence of TRPC5 in DRG lysates via Western blot and assessed the specificity of reactions via staining of *TRPC5$^{-/-}$* tissues (Fig. 2*A*, *Inset*). Size–frequency distribution demonstrated that the majority of TRPC5$^+$ neurons are small- to medium-sized, but, clearly, TRPC5 also was present in large-diameter neurons (Fig. 2*B*). We also isolated mRNA from lysates of dissociated DRG neurons and detected TRPC5 transcripts (24). TRPC5 also is present in human tissues, and immunolabeling demonstrated that TRPC5 is expressed in intraepithelial nerve endings within the human skin (Fig. 2*C*). Although regionally variable, the dorsum of the hand and the proximal forearm are innervated densely with these fibers. In peripheral nerves, ~34% of fibers in the proximal incoming processes of L5 are positive for TRPC5 (Fig. 2*D*). This proportion, and the colocalization of ~15% of fibers with TRPM8, indicates distinct fiber populations. In human DRGs, size–frequency distribution of TRPC5 positivity was similar to that observed in the mouse (~30% of DRGs). Double-labeling experiments with TRPC5 and TRPM8 also indicated distinct populations (Fig. 2*E*, *Inset*); however, colocalization studies in humans are limited by lipofuscin autofluorescence (25). In the human spinal cord, TRPC5 was most dense in the outer parts of the dorsal horn, corresponding to regions I–III of

the superficial laminae (Fig. 2*F*). Thus, the distribution of TRPC5 in the examined levels of the human and mouse peripheral sensory systems is typical of proteins involved in temperature sensing and nociception, suggesting a potential role for TRPC5 in the perception of cold and/or cold pain. Therefore, we analyzed the functional role of TRPC5 in murine sensory neurons.

Characterization of Thermally Sensitive TRPs in DRG Neurons from WT and *TRPC5$^{-/-}$* Mice. Sensory ganglia from TRPC5-deficient mice appeared structurally normal (Fig. 2 *A* and *B*), and the proportion of cells stained with antibodies to neurofilament 200 (NF200) protein (a marker of A-fiber sensory neurons) and peripherin (present in most nociceptive neurons) was not significantly different than in WT neurons (Fig. 3*A*). Similarly, the proportion of neurons containing calcitonin gene-related peptide (CGRP), important in setting heat thresholds of sensory neurons (26), and of nonpeptidergic neuronal cell bodies [labeled with isolectin B4 (IB4)] was unchanged (Fig. 3*A*). Immunophenotyping of WT and *TRPC5$^{-/-}$* DRGs showed similar proportions of TRPV1$^+$ neurons; however, TRPM8$^+$ neurons were reduced by almost half (Fig. 3 *A* and *B* and [Table S2](#)). To test whether the reduction of TRPM8 protein is related to transcript levels, we determined mRNA levels for TRPM8, TRPV1, and TRPA1 in DRG lysates but found no significant difference between WT and *TRPC5$^{-/-}$* mice. Conversely, TRPC5, TRPV1, and TRPA1 mRNA levels were unchanged from WT in *TRPM8$^{-/-}$* mice. In conjunction with previously documented TRPM8 in peripheral endings (11) and TRPC5 outgrowth to neurites (20–22), our findings suggest that TRPM8 and TRPC5 might function primarily in peripheral terminals rather than in cell bodies.

In initial behavioral tests of 129S1/SvImJ *TRPC5$^{-/-}$* mice, we found that acute pain thresholds for heat, mechanical threshold, sensitivity to noxious cold pain, and temperature preference
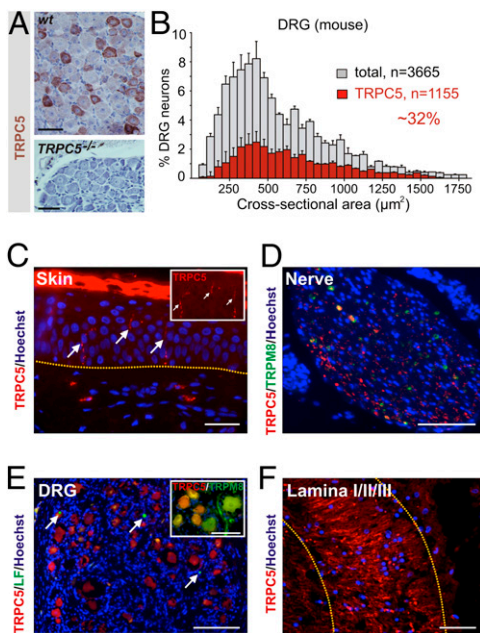
Fig. 2. TRPC5 in mouse and human peripheral nerves, DRG, and the spinal cord dorsal horn. (*A*) (*Upper*) TRPC5 is present as diffuse cytoplasmic staining in adult mouse DRG neurons. (*Lower*) TRPC5 staining in sections from *TRPC5⁻/⁻* DRGs. (*B*) Size–frequency distribution of TRPC5 in murine sensory neurons (TRPC5⁺/total neuron counts from eight DRGs: 290/687; 194/515; 169/482; 52/284; 158/451; 167/488; 37/408; and 88/350, respectively; mean diameter: 27.3 μm). Note: The majority of TRPC5⁺ neurons are small (<600 μm²) to medium-sized (<1,400 μm²). (*C*) TRPC5 is present in adult human skin intraepithelial nerves (arrows); dotted line indicates basement membrane. (*Inset*) TRPC5 channel. (*D*) Cross-section of a peripheral nerve: TRPC5 and TRPM8 are present in peripheral incoming processes from spinal nerve L5 (160 fibers TRPC5⁺, 146 fibers TRPM8⁺, 49 fibers colabeled, out of 325 fibers counted in peripheral incoming processes from three DRG neurons). (*E*) TRPC5 is present as diffuse cytoplasmic staining in adult human DRG neurons. LF, lipofuscin autofluorescence (arrows). (*Inset*) Human L5-DRG, double-labeled for TRPC5/TRPM8, contains three populations of neurons: 36% TRPM8⁺ (102/287; note the emerging fiber), 34% TRPC5⁺ (102/287 neurons), and 11% TRPM8/C5-colabeled neurons (32/287 neurons; *n* = 5 DRGs). (*F*) TRPC5⁺ is located in the adult human superficial dorsal horn, corresponding to lamina I/II/III (dotted lines). (Scale bars: *A*, *C*, *F*, and *Inset E*, 50 μm; *E*, 200 μm; *D*, 250 μm.)

behavior as well as behavior in a temperature gradient were all normal ([Fig. S2](#)). Similarly, neither acetone- nor icilin-induced writhing behavior exhibited measurable differences. We conclude that, like TRPM8, TRPC5 is not required for noxious cold sensing. The negative results on the temperature gradient preference test do not rule out TRPC5 function for sensing changes in the 37–25 °C range, because currently the understanding of the cause-and-effect relationship between sensory stimuli and behavioral responses is limited (27). Thus, we set out to investigate temperature sensing in the peripheral nervous system.

In patch clamp studies of cultured sensory ganglia or dissociated DRG neurons, we were unable to detect cold-activated I_{TRPC5}, suggesting that TRPC5 channels are down-regulated in culture, are present only in cold-insensitive C1/C5 heteromultimers, or are confined to nerve terminals. To determine whether cold sensitivity was intact in these isolated neurons, we also used ratiometric Ca^{2+} imaging of dissociated cultured DRG from WT and *TRPC5⁻/⁻* mice. When isolated neurons were cooled from 30 °C to 10 °C, intracellular Ca^{2+} increased in 16% of cells. Consistent with some prior studies (15), we found that 8% of the whole neuron population and 40% of the cold-sensitive cells were sensitive to menthol. In DRG neurons isolated from *TRPC5⁻/⁻* mice, ~70% of cold-sensitive cells were lost, and the fraction of cold-sensitive cells was reduced to ~4.6 ± 0.9% in
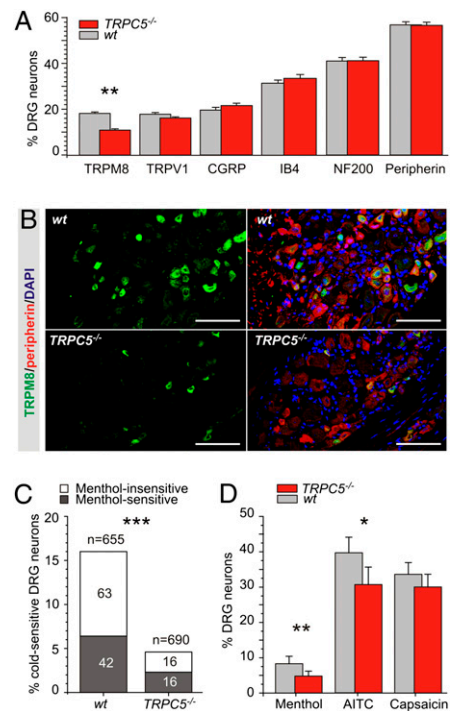
Fig. 3. Functional and immunophenotypic characterization of thermo-TRPs in DRG neurons from WT and *TRPC5⁻/⁻* mice. (*A*) Percentage of isolated DRG neurons identified by anti-TRPM8, -TRPV1, -CGRP, -peripherin, -NF200, and -IB4 antibodies. Only the percentage of TRPM8⁺ neurons was significantly different (**$P < 0.005$). (*B*) DRG were immunostained with anti-TRPM8 (green) or -peripherin (red) antibodies and DAPI nuclear staining (blue). TRPM8 expression is decreased in *TRPC5⁻/⁻* mouse DRG. (Scale bars: 50 μm.) (*C*) Comparison of cold sensitivity in WT and *TRPC5⁻/⁻* DRG neurons. WT neurons: 16% (105/655) of neurons were activated by cold, and 40% (42/105) of cold-sensitive neurons demonstrated menthol sensitivity. *TRPC5⁻/⁻* neurons: 4.6% (32/690) of neurons were activated by cold, and 50% (16/16) of cold-sensitive neurons were menthol-sensitive (***$P < 0.00001$). Note: Despite a striking reduction of cold-sensitive *TRPC5⁻/⁻* neurons, the fraction of cold-sensitive neurons that demonstrate menthol sensitivity was maintained (40% vs. 50%). (*D*) Percentage of WT (gray) and *TRPC5⁻/⁻* (red) neurons with responses to menthol (TRPM8 activator), allyl isothiocyanate (AITC) (TRPA1 activator), or capsaicin (TRPV1 activator). Fewer neurons in *TRPC5⁻/⁻* mice than in WT mice responded to menthol or allyl isothiacyanate (AITC) (**$P < 0.005$; *$P < 0.05$).

TRPC5⁻/⁻ mice (*n* = 8) compared with 16.0 ± 1.7% in WT mice (*n* = 7). These results indicate that the total number of cold-sensitive neurons and functional expression of TRPM8 were reduced in *TRPC5⁻/⁻* cultured DRG neurons. Despite the striking reduction, the fraction of cold-sensitive neurons that demonstrate menthol sensitivity was maintained (*TRPC5⁻/⁻*: 50% vs. WT: 40%; Fig. 3*C*). In contrast, the proportion of neurons expressing functional TRPV1 was similar in cells isolated from *TRPC5⁻/⁻* and WT mice (~30%), and TRPA1 was reduced only slightly (*TRPC5⁻/⁻*: 30% vs. WT: 40%; Fig. 3*D* and [Table S3](#)). Thus, dissociated neurons in culture have altered TRPM8 and TRPC5 function but maintain sensitivity to stimuli in the noxious cold range (10–15 °C). We presume that most noxious cold sensitivity is encoded via ion channels other than TRPM8 or TRPC5.

Skin-Nerve Recordings of WT and *TRPC5⁻/⁻* Mice. The dearth of reliable assays to quantify protein levels of ion channels in peripheral nerve terminals in the skin led us to assay their function in skin-nerve preparations. We compared the functional properties of C-fiber responses to cold in *TRPC5⁻/⁻* and *TRPM8⁻/⁻* mice (11, 13, 28). Skin-nerve preparations allow stimulation of isolated

receptive fields of single C- and Aδ-fibers in mouse skin while recording propagated action potentials extracellularly (29, 30). Extensive prior work in mammals established three types of cold-sensitive afferent fibers: mechanosensitive C-fibers (nociceptors, C-mechano; CM), cold receptors (C-cold; CC), and mechanosensitive Aδ-fibers (Aδ-nociceptors) (31–37). In the mouse, CM-fibers can be subdivided further into two cold-sensitive subclasses, the cold nociceptors (C-mechano cold, CMC) and the multimodal cold nociceptors (C-mechano-cold-heat, CMCH) (29). In primates, CMC- and CMCH-fibers are believed to relay information to the brain that is perceived as painful cold, whereas CC-fibers are likely associated with innocuous cold (33, 35).

We compared responses of C-fiber nociceptors to cooling of the receptive fields from 30 to ~10 °C. $TRPC5^{-/-}$ mice had a lower proportion of CMCH-fibers (<2% compared with 10% in WT mice), which appeared to be replaced by hypersensitive

CMC-fibers. Specifically, CMC-fibers in $TRPC5^{-/-}$ mice displayed a fourfold increase in response magnitude with threefold higher peak discharge rates (Fig. 4 A–D). In $TRPC5^{-/-}$ mice, 84% of CMC-fibers were sensitive to menthol compared with 38% in WT (Fig. 4 E–G and Fig. S3). In both WT and $TRPC5^{-/-}$ mice, the menthol-sensitive population of cold nociceptors contributed the majority of action potentials to the combined cold response. Significantly, this proportion increased from ~70% in WT to 95% in the $TRPC5^{-/-}$ fibers (Fig. 4 F and G). A small but significant shift of the median mechanical (Von Frey) threshold to lower values accompanied these changes (Fig. S4 A and B). However, other characteristics of CM-fibers, such as heat sensitivity and conduction velocity, remained unchanged. We interpret these data to mean that loss of TRPC5 leads to plastic changes in the response properties of CMC-fibers, most likely because of adaptation of TRPM8 or other menthol-sensitive

Fig. 4. Skin-nerve recordings of WT and $TRPC5^{-/-}$ mice: gain of function in C-cold nociceptors (CMC). C-cold nociceptors of $TRPC5^{-/-}$ mice had larger cold responses than those of WT mice as measured by action potential firing rates (A), action potentials (APs) per cold stimulus (B), and peak firing rates (C) but exhibited similar temperature thresholds (D). (E) Four-way distribution pattern of the subclasses of mechanosensitive C-fibers in WT and $TRPC5^{-/-}$ mice, identified by mechanostimulation and subsequent thermal characterization. The numbers of fibers in WT and $TRPC5^{-/-}$ cells are given in parentheses. CM, mechano-sensitive nociceptor; CMC, mechano-cold nociceptor; CMCH, mechano-cold and heat nociceptor; CMH, mechano-heat nociceptor. (F) $TRPC5^{-/-}$ mice exhibited more menthol-sensitive CMCs and fired more cold- and menthol-activated action potentials than WT mice (500 μM menthol). Numbers in bars indicate number of fibers (Left) and number of action potentials (Right). (G) Original cold response of WT and $TRPC5^{-/-}$ CMC-fibers before and after treatment with menthol (arrow); I.f.p. s^{-1}, instantaneous frequency plot. (Insets) Extracellular potentials; y = 200 μV, x = 1 ms. (H) Four-way distribution pattern of the subclasses of mechanosensitive C-fibers in WT and $TRPM8^{-/-}$ mice; compare to E. $TRPM8^{-/-}$ mice lack CMC-fibers and exhibit more CMH-fibers. (I) Menthol-insensitive Aδ-cold nociceptors were observed infrequently in $TRPC5^{-/-}$ mice, and responses were small (n = 65 each genotype). Note: The fraction of cold-sensitive fibers that demonstrate menthol sensitivity (WT: 13.3% vs. $TRPC5^{-/-}$: 33.3%) as well as responses (WT: 13.7% vs. $TRPC5^{-/-}$: 58.2%) was increased. (J) Representative responses of $TRPC5^{-/-}$ and WT Aδ-cold nociceptors; (Insets) extracellular potentials; y = 200 μV, x = 1 ms. *P < 0.05; **P < 0.0005; Mann–Whitney U test (B–D) and χ^2 test (F and I). See also SI Materials and Methods.

NEUROSCIENCE

channels and a subsequent shift in mechanosensitive C-fiber subtypes.

To test whether genetic ablation of TRPC5 results in up-regulation of TRPM8, we examined mRNA levels of pooled peripheral nerves, DRG, and trigeminal ganglia and quantified TRPM8-positive peripheral fibers by immunohistochemistry. No significant difference between WT and $TRPM8^{-/-}$ mice ($n > 8$) was found, although there was a trend toward increased numbers of TRPM8-positive fibers in $TRPC5^{-/-}$ mice (average fibers per high-power field, WT: 2.7 ± 0.4 vs. $TRPC5^{-/-}$: 3.4 ± 0.4; t test; $P = 0.059$). For comparison, we examined $TRPM8^{-/-}$ mice and found a complete lack of CMC-fibers accompanied by increased numbers of heat-sensitive C-fibers (CMH) (Fig. 4H). A significant shift of the median mechanical (Von Frey) threshold to higher values accompanied these changes (Fig. S4 C and D). In $TRPM8^{-/-}$ mice, CMCH-fibers appear at normal ratios (Table S4) and may be responsible for noxious cold sensing in the absence of TRPM8. Together, these findings suggest that noxious cold sensation does not require TRPC5 and that noxious cold sensation in $TRPM8^{-/-}$ mice is maintained by a shift from CMC- to CMCH-fibers (Fig. 4H and Table S4).

We also examined the rare unimodal cold receptors, CC (2), that frequency-encode temperature and show phasic activity upon cooling and rapid adaptation to warming (33). CC-fibers were characterized recently in the mouse cornea (35), are menthol sensitive, and exhibit 20-fold larger responses than CMC-fibers. CC-fibers in the cornea of $TRPM8^{-/-}$ mice are menthol insensitive (35), and we found no difference in CC-fiber characteristics between WT and $TRPC5^{-/-}$ mice (Fig. S5). However, a significant fraction of CC-fibers was able to encode noxious cold-stimuli (Fig. S5G).

Finally, we assessed cold-sensitive Aδ-fibers and found an overall reduction in cold-induced action potentials, from 21% in WT to 9% in $TRPC5^{-/-}$ mice, whereas the menthol-sensitive fraction was maintained in both genotypes (Fig. 4 I and J and Fig. S6). A similar reduction of cold-sensitive Aδ-fibers has been documented in $TRPM8^{-/-}$ mice (11). Note, however, that the pattern of encoding cold stimulus intensity in murine Aδ-fibers is different from that in primates, and the significance of alterations in this fiber type is currently unknown (33, 37).

Discussion

The most surprising finding of this study is that TRPC5 monomeric channels have high gating sensitivity to cooling in the range from 37–25 °C. As expected, this effect is strongly potentiated by Gq-linked G protein–coupled receptors. Interestingly, TRPC1/C5 heteromeric channels did not display strong cold sensitivity. Exceptionally high temperature sensitivities in ion channel gating likely result from large changes in molar heat capacity, but these changes can be accounted for by relatively few residues within a domain or distributed throughout the protein. One likely scenario is that hydrophobic residues exposed to water during gating of TRPC5 are made inaccessible when TRPC5 forms a complex with TRPC1.

The ability to occlude TRPC5 cold sensitivity by multimerization is an interesting adaptation and is unlike previous paradigms in TRP-channel temperature-sensing biology. TRPC1/TRPC5 heteromers presumably are confined to cell bodies, whereas TRPC5 is targeted to distal processes (20–22). Thus, TRPC5, which is highly sensitive to mild cooling, is expected to increase depolarization in distal processes but not in cell bodies. This targeting may confine the neuronal response to cooling to the periphery, leading to increased intracellular calcium in these processes. The findings presented here suggest that these changes are not sensed by the central nervous system in ways leading to appreciable changes in behavior. However, they may lead to changes in neurite outgrowth, local vascular perfusion, or other cellular adaptation such as up-regulation of other channel types.

We emphasize the distinction between avoidance behavior to noxious cold and thermal preference behavior from other biological adaptations. Although temperature sensing is such a common experience that we tend to attribute temperature changes to conscious recognition, all biological processes are temperature dependent, and most are not reported to the nervous system. In this context, we postulate that the heightened sensitivity of TRPC5 to cooling is used for other adaptations, such as localized metabolic changes, vascular changes, retraction of neurites, or initiation of transcriptional programs. Our findings suggest that TRPC5 activation may be potentiated by PLC-coupled receptors, such as growth factors, as well as by Gq-linked receptors. Indeed, in reptiles and mammals long-term exposure to various temperatures results in impressive long-lasting adaptive changes in the firing properties of innocuous thermosensors (38, 39). Another explanation would be that deleting TRPC5 results in compensatory replacement by functionally overlapping cold transducers (e.g., TRPM8). Increased functional availability of TRPM8 then may account for the avoidance of cold temperatures by $TRPC5^{-/-}$ mice. Reminiscent of our findings in $TRPC5^{-/-}$ mice, the compensatory replacement of functionally related tetrodotoxin-sensitive ion channels in Nav1.8-deficient mice (40) partially restored the loss of Nav1.8 function in the null-mutant nerve endings but not in their cultured DRG neurons (30, 41). In both cases, the result is protection from cold via functionally overlapping but molecularly independent cold-detection mechanisms.

In summary, we found that innocuous cold-responsive TRPC5 is present in approximately one-third of mouse sensory neurons as well as in a substantial number of human peripheral nerves. In agreement with previous work demonstrating targeting of TRPC5 to neurites (21), we failed to measure TRPC5 currents in isolated neurons lacking neurites. Given that DRG neurons are pseudounipolar and that propagation of cell soma action potential is not required for transmission from the periphery to the spinal cord, we hypothesized that most TRPC5 homomeric channels are targeted to nerve terminals that are inaccessible to direct recording. To determine whether this idea is functionally relevant, we conducted behavioral tests and found no differences between WT and $TRPC5^{-/-}$ mice in various temperature-sensing assays, suggesting a role for TRPC5 that is distinct from noxious cold sensing. However, several limitations apply to our results. First, it is not clear whether cold-induced activation of TRPC5 contributes directly to propagation of action potentials along the sensory pathway. Second, we used 129S1/SvImJ mice in these studies, and this strain may be inferior to C57BL/6 mice in behavioral assays (42, 43). It has been noted that there are temperature-sensing differences between mouse strains (44, 45), and we cannot generalize our results to other strains or species.

Despite these limitations, we found that loss of TRPC5 resulted in significant adaptive responses. In isolated neurons, these changes resulted in a significant drop in the percentage of cold-sensitive (both menthol-sensitive and methol-insensitive) DRG neurons and TRPM8 detected by antibody. Interestingly the fraction of cold-sensitive neurons demonstrating menthol sensitivity was maintained, and loss of TRPC5 did not result in changes in CGRP, IB4, NF200, peripherin, or TRPV1 protein. Paradoxically, in intact animals, TRPM8 and/or other menthol-sensitive channels appear to underpin a much larger component of noxious cold sensing after TRPC5 deletion, resulting in a subsequent shift in mechanosensitive C-fiber subtypes. In future experiments, it will be important to examine changes in nerve terminals, including axon outgrowth and guidance, blood flow, tissue architecture near nerve endings, and responses to both growth factors and Gq-linked receptors in $TRPC5^{-/-}$ mice to understand the specific role of TRPC5 in the innocuous range of cold temperature (37–25 °C) that evidently is distinct from noxious cold sensing.

Materials and Methods

Animals and Behavioral Assays. Mice were housed in a 12-h light-dark cycle at room temperature, and experiments were performed under the policies of the International Association for the Study of Pain and approved by the Animal Resources of Children's Hospital Boston facility. Standard sensory assays included paw flick, cold plate, von Frey thresholds, and temperature

choice assays. Behavioral studies were carried out with paired littermates while blind to genotype or (for temperature preference behavior) were videotaped and analyzed by automated detection software. See *SI Materials and Methods* for details.

DRG Neuronal Cultures and Ca²⁺ Measurements. Calcium imaging/patch clamp recordings were made using DRGs from all spinal levels after ~15–18 h in culture. For calcium imaging, DRGs were loaded with Fura2-AM (Invitrogen) dissolved in TNB medium (for 60–70 min) followed by a 15-min wash in TNB medium. Cells were considered menthol- (250 μM), capsaicin- (10 μM), or allyl-isothiocyanate- (100 μM) responsive when Ca^{2+} increased >25% above baseline. Cells were considered cold-sensitive when Ca^{2+} increased >15% above baseline (apparent Ca^{2+} fluorescence decreased in cold-insensitive cells during cold stimulation by 5–10%).

Patch Clamp Recordings. The extracellular solution contained (in mM): 140 NaCl, 5 KCl, 2 CaCl₂, 1 MgCl₂, 10 Hepes, and 10 glucose (adjusted to pH 7.4 with NaOH). The pipette (intracellular) solution contained (in mM): 120 CsMES, 10 Cs₄-BAPTA, 10 Hepes, 2 MgATP, 0.4 Na₂GTP, 0.47 MgCl₂, and 3.26 CaCl₂. Whole-cell recordings were acquired at 5 kHz and were low-pass filtered (eight-pole Bessel) at 2 kHz. Temperature coefficients (Q_{10}) were estimated by plotting log (I/I_{max}) vs. temperature. Statistical data are presented as mean ± SEM; Student's *t* test was calculated, and $P < 0.05$ was considered statistically significant.

Single Nerve Fiber Electrophysiology. The isolated skin saphenous nerve preparation and single-fiber recording technique was used (29, 30) on male littermates of WT and TRPC5⁻/⁻ mice (*n* = 32) weighing 20–32 g and on 129S1/SvImJ mice (*n* = 17; Jackson Labs). *TRPM8⁻/⁻* mice were from Ajay Dhaka and Ardem Patapoutian (Department of Cell Biology, The Scripps Research Institute, La Jolla, CA). Recordings were performed from male mice (*n* = 10) backcrossed on N5 (F1-F2) generations to C57BL/6 background and from corresponding male littermates (*n* = 11).

Immunohistochemistry. Cryostat- or paraffin-embedded sections of 3- to 8-μM thickness were prepared from fresh-frozen or paraformaldehyde-fixed (4%) tissues, respectively. Quantification of labeled cells was assessed blinded to genotype and according to previously published protocols (46, 47).

1. Bessou P, Perl ER (1969) Response of cutaneous sensory units with unmyelinated fibers to noxious stimuli. *J Neurophysiol* 32:1025–1043.
2. Zotterman Y (1936) Specific action potentials in the lingual nerve of the cat. *Skand Arch Physiol* 75:105–119.
3. Kang D, Choe C, Kim D (2005) Thermosensitivity of the two-pore domain K+ channels TREK-2 and TRAAK. *J Physiol* 564:103–116.
4. Ramsey IS, Moran MM, Chong JA, Clapham DE (2006) A voltage-gated proton-selective channel lacking the pore domain. *Nature* 440:1213–1216.
5. Caterina MJ, Rosen TA, Tominaga M, Brake AJ, Julius D (1999) A capsaicin-receptor homologue with a high threshold for noxious heat. *Nature* 398:436–441.
6. Caterina MJ, et al. (1997) The capsaicin receptor: A heat-activated ion channel in the pain pathway. *Nature* 389:816–824.
7. Xu H, et al. (2002) TRPV3 is a calcium-permeable temperature-sensitive cation channel. *Nature* 418:181–186.
8. Peier AM, et al. (2002) A TRP channel that senses cold stimuli and menthol. *Cell* 108:705–715.
9. Fajardo O, Meseguer V, Belmonte C, Viana F (2008) TRPA1 channels mediate cold temperature sensing in mammalian vagal sensory neurons: Pharmacological and genetic evidence. *J Neurosci* 28:7863–7875.
10. Story GM, et al. (2003) ANKTM1, a TRP-like channel expressed in nociceptive neurons, is activated by cold temperatures. *Cell* 112:819–829.
11. Bautista DM, et al. (2007) The menthol receptor TRPM8 is the principal detector of environmental cold. *Nature* 448:204–208.
12. Colburn RW, et al. (2007) Attenuated cold sensitivity in TRPM8 null mice. *Neuron* 54:379–386.
13. Dhaka A, et al. (2007) TRPM8 is required for cold sensation in mice. *Neuron* 54:371–378.
14. Karashima Y, et al. (2009) TRPA1 acts as a cold sensor in vitro and in vivo. *Proc Natl Acad Sci USA* 106:1273–1278.
15. Munns C, AlQatari M, Koltzenburg M (2007) Many cold sensitive peripheral neurons of the mouse do not express TRPM8 or TRPA1. *Cell Calcium* 41:331–342.
16. Clapham DE (2003) TRP channels as cellular sensors. *Nature* 426:517–524.
17. Ramsey IS, Delling M, Clapham DE (2006) An introduction to TRP channels. *Annu Rev Physiol* 68:619–647.
18. Blair NT, Kaczmarek JS, Clapham DE (2009) Intracellular calcium strongly potentiates agonist-activated TRPC5 channels. *J Gen Physiol* 133:525–546.
19. Rohács T, Lopes CM, Michailidis I, Logothetis DE (2005) PI(4,5)P2 regulates the activation and desensitization of TRPM8 channels through the TRP domain. *Nat Neurosci* 8:626–634.
20. Strübing C, Krapivinsky G, Krapivinsky L, Clapham DE (2001) TRPC1 and TRPC5 form a novel cation channel in mammalian brain. *Neuron* 29:645–655.
21. Bezzerides VJ, Ramsey IS, Kotecha S, Greka A, Clapham DE (2004) Rapid vesicular translocation and insertion of TRP channels. *Nat Cell Biol* 6:709–720.
22. Greka A, Navarro B, Oancea E, Duggan A, Clapham DE (2003) TRPC5 is a regulator of hippocampal neurite length and growth cone morphology. *Nat Neurosci* 6:837–845.
23. Gomis A, Soriano S, Belmonte C, Viana F (2008) Hypoosmotic- and pressure-induced membrane stretch activate TRPC5 channels. *J Physiol* 586:5633–5649.
24. Wu D, Huang W, Richardson PM, Priestley JV, Liu M (2008) TRPC4 in rat dorsal root ganglion neurons is increased after nerve injury and is necessary for neurite outgrowth. *J Biol Chem* 283:416–426.
25. Holford LC, Case P, Lawson SN (1994) Substance P, neurofilament, peripherin and SSEA4 immunocytochemistry of human dorsal root ganglion neurons obtained from post-mortem tissue: A quantitative morphometric analysis. *J Neurocytol* 23:577–589.
26. Mogil JS, et al. (2005) Variable sensitivity to noxious heat is mediated by differential expression of the CGRP gene. *Proc Natl Acad Sci USA* 102:12938–12943.
27. Devor M (2008) Nociception in Kyoto. *Pain* 140(3):519–520; author reply 520–511.
28. Riccio A, et al. (2009) Essential role for TRPC5 in amygdala function and fear-related behavior. *Cell* 137:761–772.
29. Zimmermann K, et al. (2009) Phenotyping sensory nerve endings in vitro in the mouse. *Nat Protoc* 4:174–196.
30. Zimmermann K, et al. (2007) Sensory neuron sodium channel Nav1.8 is essential for pain at low temperatures. *Nature* 447:855–858.
31. Hensel H, Zotterman Y (1951) The response of mechanoreceptors to thermal stimulation. *J Physiol* 115:16–24.
32. Hensel H, Zotterman Y (1951) The response of the cold receptors to constant cooling. *Acta Physiol Scand* 22:96–105.
33. Kenshalo DR, Duclaux R (1977) Response characteristics of cutaneous cold receptors in the monkey. *J Neurophysiol* 40:319–332.
34. Kress M, Koltzenburg M, Reeh PW, Handwerker HO (1992) Responsiveness and functional attributes of electrically localized terminals of cutaneous C-fibers in vivo and in vitro. *J Neurophysiol* 68:581–595.
35. Parra A, et al. (2010) Ocular surface wetness is regulated by TRPM8-dependent cold thermoreceptors of the cornea. *Nat Med* 16:1396–1399.
36. Reeh PW (1986) Sensory receptors in mammalian skin in an in vitro preparation. *Neurosci Lett* 66:141–146.
37. Simone DA, Kajander KC (1997) Responses of cutaneous A-fiber nociceptors to noxious cold. *J Neurophysiol* 77:2049–2060.
38. Hensel H, Schäfer K (1982) Static an dynamic activity of cold receptors in cats after long-term exposure to various temperatures. *Pflugers Arch* 392:291–294.
39. Hensel H, Schäfer K (1981) Activity of warm receptors in Boa constrictor raised at various temperatures. *Pflugers Arch* 392:95–98.
40. Matsutomi T, Nakamoto C, Zheng T, Kakimura J, Ogata N (2006) Multiple types of Na(+) currents mediate action potential electrogenesis in small neurons of mouse dorsal root ganglia. *Pflugers Arch* 453:83–96.
41. Akopian AN, et al. (1999) The tetrodotoxin-resistant sodium channel SNS has a specialized function in pain pathways. *Nat Neurosci* 2:541–548.
42. Royce JR (1972) Avoidance conditioning in nine strains of inbred mice using optimal stimulus parameters. *Behav Genet* 2:107–110.
43. Royce JR, Yeudall LT, Poley W (1971) Diallel analysis of avoidance conditioning in inbred strains of mice. *J Comp Physiol Psychol* 76:353–358.
44. Huang SM, Li X, Yu Y, Wang J, Caterina MJ (2011) TRPV3 and TRPV4 ion channels are not major contributors to mouse heat sensation. *Mol Pain* 7:37.
45. Mogil JS, et al. (1999) Heritability of nociception I: Responses of 11 inbred mouse strains on 12 measures of nociception. *Pain* 80:67–82.
46. Hager UA, et al. (2008) Morphological characterization of rat Mas-related G-protein-coupled receptor C and functional analysis of agonists. *Neuroscience* 151:242–254.
47. Lennerz JK, et al. (2008) Calcitonin receptor-like receptor (CLR), receptor activity-modifying protein 1 (RAMP1), and calcitonin gene-related peptide (CGRP) immunoreactivity in the rat trigeminovascular system: Differences between peripheral and central CGRP receptor distribution. *J Comp Neurol* 507:1277–1299.

NEUROSCIENCE